JOURNAL OF VIROLOGY, Sept. 1995, p. 5599–5606 Vol. 69, No. 9
0022-538X/95/$04.00+0

The Neurovirulent GDVII Strain of Theiler's Virus Can Replicate in Glial Cells

J. PEDRO SIMAS, HEATHER DYSON, AND JOHN K. FAZAKERLEY*

Department of Pathology, Cambridge University, Cambridge CB2 1QP, United Kingdom

Received 18 January 1995/Accepted 7 June 1995

The distribution, spread, neuropathology, tropism, and persistence of the neurovirulent GDVII strain of Theiler's virus in the central nervous system (CNS) was investigated in mice susceptible and resistant to chronic demyelinating infection with TO strains. Following intracerebral inoculation, the virus spread rapidly to specific areas of the CNS. There were, however, specific structures in which infection was consistently undetectable. Virus spread both between adjacent cell bodies and along neuronal pathways. The distribution of the infection was dependent on the site of inoculation. The majority of viral RNA-positive cells were neurons. Many astrocytes were also positive. Infection of both of these cell types was lytic. In contrast, viral RNA-positive oligodendrocytes were rare and were observed only in well-established areas of infection. The majority of oligodendrocytes in these areas were viral RNA negative and were often the major cell type remaining; however, occasional destruction of these cells was observed. No differences in any of the above parameters were observed between CBA and BALB/c mice, susceptible and resistant, respectively, to chronic CNS demyelinating infection with TO strains of Theiler's virus. By using Southern blot hybridization to detect reverse-transcribed PCR-amplified viral RNA sequences, no virus persistence could be detected in the CNS of immunized mice surviving infection with GDVII. In conclusion, the GDVII strain of Theiler's murine encephalomyelitis virus cannot persist in the CNS, but this is not consequent upon an inability to infect glial cells, including oligodendrocytes.

Theiler's murine encephalomyelitis virus (TMEV), a naturally occurring enteric pathogen of mice, is a picornavirus belonging to the *Cardiovirus* genus (30, 32, 36). Two subgroups are recognized on the basis of neurovirulence after intracerebral (i.c.) inoculation (25). One subgroup consists of TO (Theiler's original) virus strains which after i.c. inoculation, depending on the mouse strain, cause a persistent demyelinating infection of the central nervous system (CNS) in a proportion of mice that survive acute infection (21, 25, 47). Examples of TO virus strains are BeAn, DA, and WW. Mouse strains exhibit differential susceptibility to this chronic infection; SJL/J and PL/J mice are highly susceptible, and BALB/c and C57BL/6 mice are resistant. CBA mice show intermediate susceptibility. During persistent chronic infection, TO virus strains infect glial cells and give rise to lesions of demyelination (1, 3, 9, 10, 25, 39, 44). The GDVII and FA strains, the second subgroup, are highly neurovirulent and produce a fulminant encephalomyelitis in mice of all genetic backgrounds. Clinically, the mice exhibit circling behavior, breathing difficulties, ruffled fur, and flaccid paralysis culminating in death (31, 48).

During CNS infection, GDVII replicates in neurons, leading to widespread necrosis and extensive mononuclear cell inflammatory infiltrates (27, 44). GDVII has never been demonstrated in white matter, and in vivo infection of glial cells has not been studied. An intriguing question is whether GDVII infects glial cells and can produce a persistent infection. Infectivity studies of mice given sublethal doses of GDVII have failed to convincingly demonstrate any viral persistence in the CNS (26). Studies of recombinant GDVII and TO viruses have sought to map phenotypic properties of TMEV to genetic loci. Elucidation of the genetic determinants of neurovirulence, persistence, and demyelination has proved difficult and controversial (17, 18, 20, 24, 41, 46). Persistence is likely to be governed by a variety of factors including viral tropism and immune responses. In vitro, GDVII has been shown to infect and cause demyelination in organotypic CNS cultures (42) and to lytically infect cells in mixed glial cell cultures and cultures of Schwann cells (16, 29). However, the in vivo tropism of GDVII has not been subjected to detailed study. In this study, we have investigated the distribution, spread, neuropathology, and tropism of GDVII following infection of CBA and BALB/c mice. The ability of GDVII to establish a persistent infection of the CNS in CBA mice was also investigated.

* Corresponding author. Present address: Department of Veterinary Pathology, Royal School of Veterinary Studies, Summerhall, Edinburgh EH9 1QH, Scotland, UK. Phone: 131 650 6160. Fax: 131 650 6511.

MATERIALS AND METHODS

Viruses and animals. The GDVII strain of TMEV was a gift from H. Lipton (Mount Sinai Medical Center, New York, N.Y.). Virus was grown in BHK-21 cells cultured in Glasgow's modified Eagle's medium (GMEM) supplemented with 10% newborn calf serum and tryptose phosphate broth. Culture supernatants containing infectious virus were aliquoted and stored at −70°C. Four- to 6-week-old CBA and BALB/c mice were obtained from the Department of Pathology Animal Unit (Cambridge University, Cambridge, United Kingdom) and Olac (Bicester, United Kingdom). Mice were anesthetized, and 10^4 PFU of virus in 20 μl of phosphate-buffered saline (PBS) was inoculated i.c. in the region of the limbic or occipital cortex, close to the midline. Mice were euthanized at various times, and CNS tissues were removed. The brains were divided sagittally, and the spinal cords were divided laterally or longitudinally. The brain and cord halves were either processed for RNA extraction, frozen for virus titration, or fixed in 10% phosphate-buffered formalin for histological studies. Fixed tissues were dehydrated and embedded in paraffin. The brains were cut sagittally close to the midline, and the spinal cords were cross-sectioned in seven different areas. Sections, 5 μm thick, were mounted on poly-L-lysine- or Biobond (British Biocell)-coated slides.

Virus titers. Infectious virus was quantified by plaque assay on BHK-21 cell monolayers. CNS tissues were weighed and homogenized, 1:5 and 1:10 (wt/vol) for brains and spinal cords, respectively, in GMEM with 20 mM HEPES (*N*-2-hydroxyethylpiperazine-*N*′-2-ethanesulfonic acid) buffer. Tenfold dilutions of homogenized tissues or supernatant aliquots from mixed glial cell cultures were added to PBS-washed cell monolayers and incubated for 45 min at room temperature. Monolayers were then overlaid with 1% agar in GMEM supplemented with 10% bovine serum albumin (BSA), incubated for 3 days at 37°C, fixed in 10% formalin, and stained with toluidine blue, and the plaques were enumerated. Virus titers were expressed as PFU per gram of CNS tissue or PFU per

milliliter of culture supernatant. The limits of detection of the plaque assay were $10^{1.7}$ and 10^2 PFU/g for brain and spinal cord tissues, respectively.

Peripheral immunization with heat-inactivated GDVII. GDVII was heat inactivated at 65°C for 1 h, after which no infectivity remained as determined by plaque assay. CBA mice (3 to 4 weeks old) were primed with complete Freund's adjuvant containing heat-inactivated GDVII (2:1); each mouse received 10^6 to 10^7 PFU in 100 μl subcutaneously in the base of the tail. After 2 weeks, the mice were boosted with incomplete Freund's adjuvant–heat-inactivated GDVII (2:1) subcutaneously in the flank.

In situ hybridization. Riboprobes were transcribed from a recombinant pGEM 3 vector into which we had subcloned the 3.4-kb, *Sal*I-*Xba*I restriction fragment of the cDNA of the BeAn strain of TMEV, corresponding to nucleotides 1729 to 4733 on the BeAn infectious clone (35). Riboprobes were labelled either with ^{35}S-ATP and ^{35}S-CTP or with digoxigenin-UTP. In situ hybridization was performed as previously described (43). Briefly, after permeabilization, prehybridization was performed at 55°C for 1 h in a mixture of 50% deionized formamide, 5× Denhardt's solution, 0.1% sodium dodecyl sulfate, 0.75 M NaCl, 0.025 M PIPES [piperazine-*N*-*N*′-bis(2-ethanesulfonic acid)], 0.025 M EDTA, 500 μg of sonicated salmon sperm DNA per ml, 250 μg of yeast tRNA per ml and 20 U of heparin per ml. Hybridization in the same solution with the addition of 10% dextran sulfate was performed overnight at 55°C. Stringency washes with 2× SSC (1× SSC is 0.15 M NaCl plus 0.015 M sodium citrate) and 0.2× SSC were carried out for 15 min at 37 and 55°C, respectively. For ^{35}S-labelled riboprobes, sections were dehydrated, air dried, and exposed to high-resolution β-max film (Amersham, Amersham, United Kingdom) before being dipped in photographic emulsion. The length of exposure was from 4 to 7 days, as appropriate. Finally, slides were developed and conterstained with hematoxylin and eosin. For digoxigenin-labelled riboprobes, slides were incubated with sheep anti-digoxigenin immunoglobulin G conjugated to alkaline phosphatase (Boehringer Mannheim), and the reaction was visualized by using nitroblue tetrazolium and X-phosphate to give a blue product. Alternatively, digoxigenin probes were visualized by using an avidin-biotin-peroxidase kit, with sheep anti-digoxigenin immunoglobulin G and biotinylated goat anti-sheep immunoglobulin G and diaminobenzidine as the substrate, giving a brown reaction product.

Immunostaining and double labelling. Immunostaining of paraffin-embedded sections was performed as described previously (44). Briefly, sections were deparaffinized; treated with 0.3% hydrogen peroxide; rehydrated; incubated for 2 h at room temperature with a primary antibody, either rabbit polyclonal anti-bovine glial fibrillary acidic protein (GFAP) (Dakopatt) or rabbit polyclonal anti-bovine 2′,3′-cyclic-nucleotide-3′-phosphohydrolase (CNPase) (a kind gift from F. A. McMorris [38]); and then incubated for 1 h at room temperature with a secondary biotinylated goat anti-rabbit IgG (Vector Laboratories). The signal was amplified by using a Vector Laboratories ABC kit according to the manufacturer's instructions, and virus-positive cells were visualized by using diaminobenzidine as the substrate. For double-labelling in situ hybridization for viral RNA, the use of a ^{35}S-labelled riboprobe was followed by immunostaining for phenotypic markers. After dehydration of the sections following the final SSC washes in the in situ hybridization procedure, the sections were immunostained, starting with 0.3% hydrogen peroxide. After immunostaining, the slides were dipped in photographic emulsion and counterstained as described above.

RNA preparation. Total RNA was extracted from the brain and spinal cord tissues of infected mice and infected BHK monolayers by the guanidine thiocyanate method as described previously (29). GDVII RNA was prepared from purified virus as described previously (8, 44). The concentration of RNA was calculated from the A_{260} value and used to standardize the reverse transcription (RT)-PCR.

RT-PCR. RT-PCR was performed by using a GeneAmp thermostable rTth RT RNA PCR kit (Perkin-Elmer Cetus) as previously described (44). Briefly, RT was performed with 100 ng of total CNS (brain and spinal cord) RNA with a 23-mer oligonucleotide primer complementary to nucleotides 3883 to 4005 of the GDVII strain of TMEV (35). After first-strand cDNA synthesis, a 17-mer upstream primer corresponding to nucleotides 3081 to 3098 of the GDVII strain of TMEV (35) was added, and the reaction mixture was subjected to 35 cycles of amplification (94 and 55°C for 20 s each, followed by 60°C for 60 s) in a Techne PHC-3 thermal cycler. The PCR products (1/10 of the reaction mix) were added to a 1% agarose gel and analyzed by Southern blot with digoxigenin probes detected by enhanced chemiluminescence (44).

RESULTS

Clinical disease and CNS virus titers. The course of virus replication in the CNS was determined for GDVII in both CBA and BALB/c mice. Three animals of each strain were sampled at days 1, 2, 3, 4 and 5 postinfection. The animals started to die at 3 days, with signs of acute encephalomyelitis, which included circling behavior, dyspnea, ruffled fur, and flaccid paralysis. All mice were dead by 5 days postinfection. Infectivity titers (Fig. 1) were equivalent in CBA and BALB/c mice. Virus titers in the brain increased rapidly and steadily, reaching maximum values within 3 days of infection. Virus titers in the spinal cord increased with time but showed more variability than those in the brain.

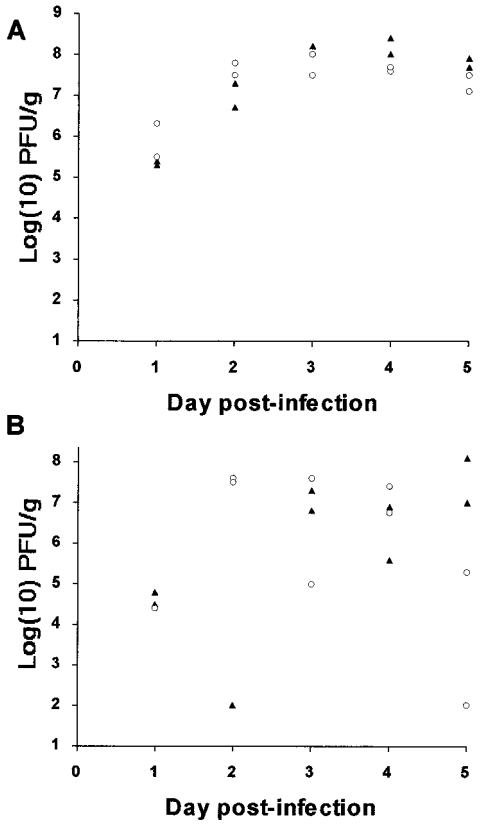

FIG. 1. Brain (A) and spinal cord (B) virus titers from CBA (closed triangles) and BALB/c (open circles) mice inoculated i.c. with 10^4 PFU of GDVII.

CNS virus distribution and spread. The temporal course of GDVII RNA distribution in the CNS of CBA and BALB/c mice was determined. Three adjacent sections from each of two animals from each strain at each time point were studied by in situ hybridization and autoradiographic analysis. The same sections were then dipped in photographic emulsion and examined microscopically. The specificity of the riboprobe was tested on age-matched, noninfected and Semliki Forest virus-infected mouse CNS tissues (14). No positive signal was detected in any of the control tissues. Representative autoradiographic images are shown in Fig. 2. There was no difference in the distributions of GDVII RNA in CBA and BALB/c mice. Virus was first apparent as small foci at 1 day postinfection and spread rapidly from these sites. By the time of death, a consistent pattern of infection, which included the cerebral cortex (predominantly the deep layers), pyramidal neurons of the hippocampus, basal ganglia, hypothalamus, substantia nigra, pons, and spinal cord grey matter, was established. No virus-positive cells were detected in the corpus callosum, cerebellum, dentate gyrus, or molecular layer of the hippocampus, which were consistently negative for virus even when surrounding cells were positive (Fig. 2 and 3). The spread of infection to outer cortical layers, inferior and superior colliculi, central thalamic nuclei, and the brain stem was rare.

The rapid spread of infection, adjacent virus-positive cell bodies, and the presence of viral genomes in neuronal processes and in certain connected nuclei indicate rapid cell-to-

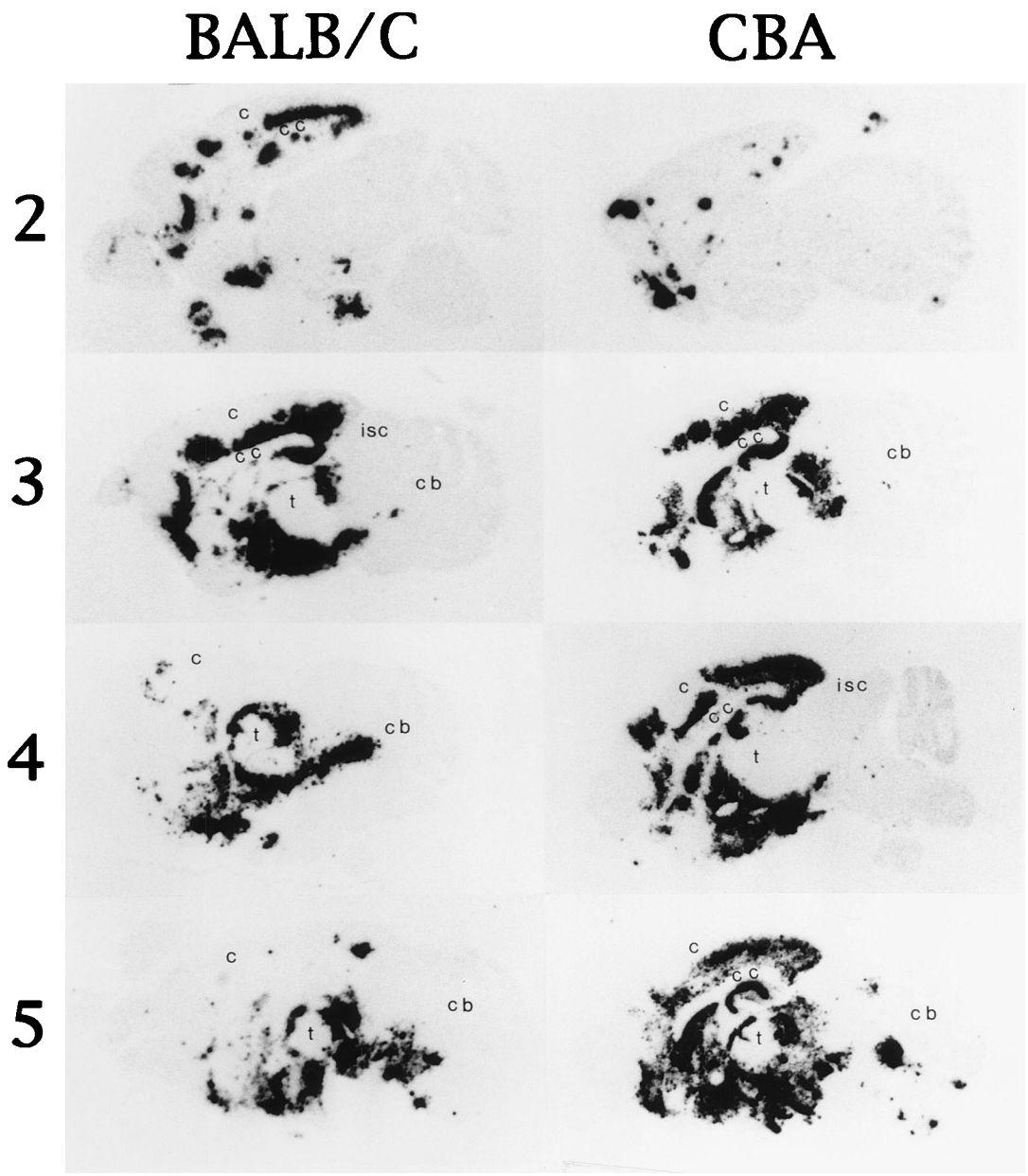

FIG. 2. Representative autoradiographic images showing temporal changes in GDVII RNA distribution in CNS of mice. In situ hybridization on sagittal and transverse sections of brain and spinal cord, respectively, with a ^{35}S-labelled riboprobe complementary to the viral genomic RNA. Note the absence of signals in the corpus callosum (cc), cerebellum (cb), central thalamic nuclei (t), inferior and superior colliculi (isc), and outer layers of the neocortex (c).

cell spread between both adjacent and distant but connected cells. Cortical neurons in layers IV, V, and VI were frequently infected. Layer V neurons project to the superior colliculus, basal ganglia, hypothalamus, and spinal cord via the internal capsule, while layers IV and VI neurons project to thalamic nuclei. That the basal ganglia, hypothalamus, spinal cord, and dentate gyrus were infected but not the superior colliculus or hippocampal pyramidal neurons suggests either that virus cannot disseminate along certain pathways or that subpopulations of neurons differ in their ability to be infected or to sustain virus replication or both. To investigate whether the consistent absence of viral RNA in specific structures represented an inability to reach, infect, or replicate within these areas, 10^4 PFU of GDVII virus was inoculated directly into the cerebella of CBA mice. Histological examination at 2 and 4 days postinoculation demonstrated destructive infection of granule and Purkinje cells (Fig. 3B), with spread of infection to the areas described above.

One striking feature of the autoradiographic analysis of the distribution of viral RNA-positive cells in the brains and spinal cords was the rarity of signal over white matter tracts such as the corpus callosum, internal capsule, and cerebellar peduncle (Fig. 3). These were consistently virus negative on autoradiographic images despite widespread infection in adjacent tissue (Fig. 2 and 3). A similar picture was observed following the exposure of sections to photographic emulsion for 7 days and microscopic examination. At boundaries between white and grey matter, for example, at the junction of cortex and corpus callosum, many virus-positive cells in the grey matter were surrounded by the strong precipitation of silver grains while

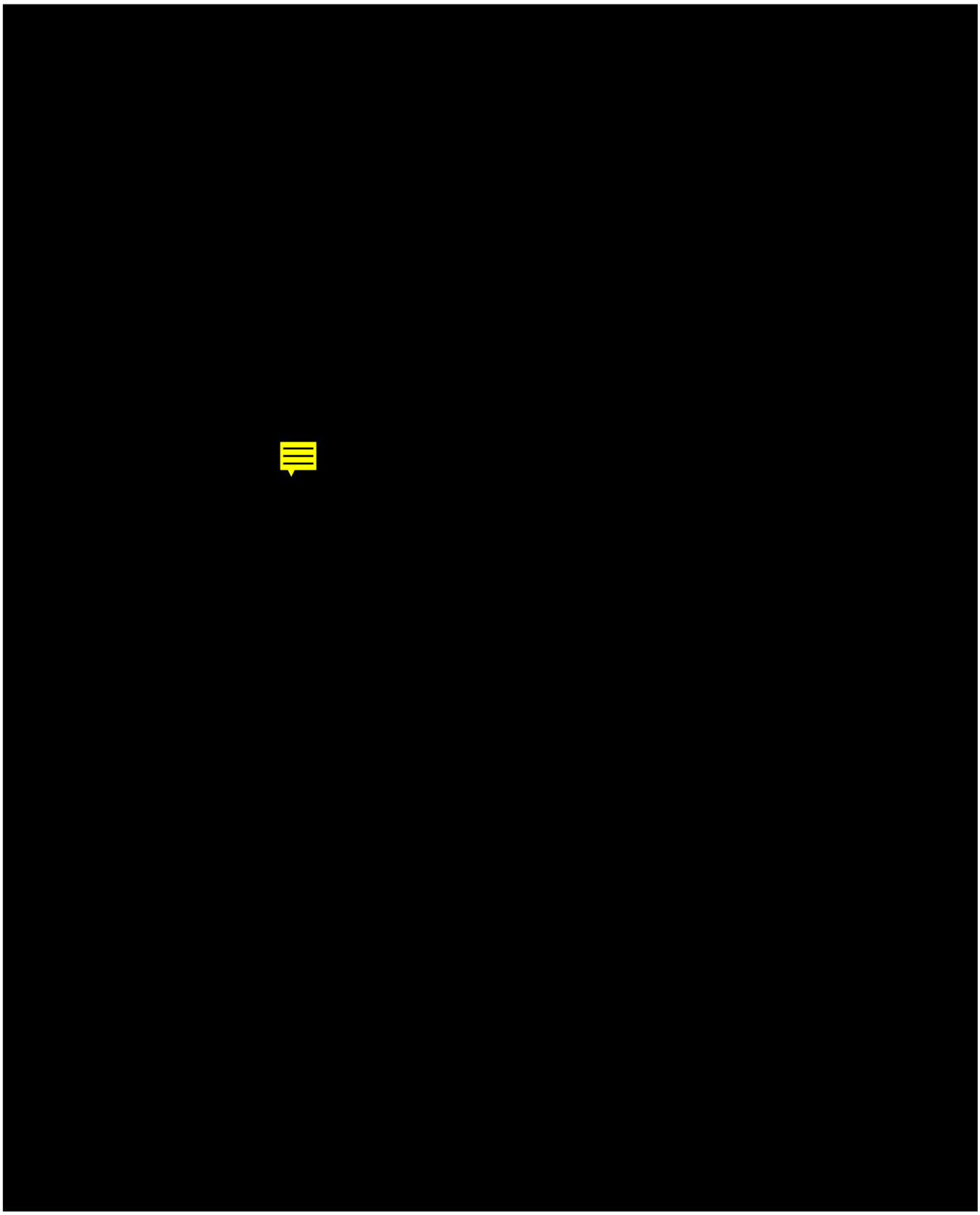

FIG. 3. Representative photomicrographs illustrating the histopathology and tropism of GDVII infection in the CNS of CBA and BALB/c mice at 3 or 4 days postinfection. All sections were 5 μm from paraffin-embedded material. GDVII RNA-positive cells were detected by in situ hybridization with a riboprobe labelled with ^{35}S or digoxigenin and visualized, respectively, by exposure to photographic emulsion (E to J, L, M, and Q) or by antibody detection using nitroblue tetrazolium and X-phosphate (A) or diaminobenzidine to give a brown reaction product (B, C, D, K, O, and P). ^{35}S in situ hybridization for viral RNA was followed by immunostaining for cell phenotypic markers with antibodies to CNPase for oligodendrocytes (E to J) and to GFAP for astrocytes (L and M). (A) GDVII RNA-positive cells with typical neuronal morphology in cerebral cortex. Staining is exclusively cytoplasmic with viral RNA present in cell processes (arrowhead). (B) Destructive infection of granule

cells in the adjacent white matter were virus negative. However, in the white matter of some mice, isolated, scattered, single virus-positive cells were occasionally observed (Fig. 3Q).

Histopathology and viral tropism. The gross appearance of the brain and spinal cord tissues in moribund mice was watery and soft. At days 1 and 2 postinfection, submeningeal and perivascular inflammatory infiltrates consisting of mononuclear and polymorphonuclear cells were observed. Viral infection was usually limited to the vicinity of the needle track. On days 3 to 5 postinfection, an acute viral encephalomyelitis with infiltrating mononuclear cells was observed. Meningitis was mild. Mononuclear perivascular inflammatory exudates were extensive, and in some mice scattered polymorphonuclear cells were present (Fig. 3R). With time, increasing numbers of cells in the areas of infection showed degenerative changes or had undergone cell death (Fig. 3D, H, J, M, and P). Degenerative changes included smaller sizes, abnormal shapes, and more-intense staining of the cytoplasm and nucleus. Pycnotic and karyorhexic nuclei were present (Fig. 3D, H, and P). Areas of extensive cell death were characterized by chromatolysis, mononuclear inflammation, and, in some cases, vacuolation of the neuropil. In areas of infection, GFAP staining demonstrated astrocytosis and astrocyte hypertrophy. Microglial proliferation was present as evidenced by cells with small basophilic, rod-shaped nuclei and occasional neuronophagia (Fig. 3K).

Some GDVII RNA-positive or GDVII protein-positive cells could be clearly identified as neurons, including motor neurons in the spinal cord and pyramidal neurons of the hippocampus (Fig. 3C, D, and O). In addition, infected cells with a distinct neuronal morphology were observed throughout the CNS (Fig. 3A). Consistent with the known site of replication of this RNA virus, viral RNA was detected in the cytoplasm but never in the nucleus (Fig. 3A). Many virus-positive neurons showed degenerative changes or cell death. For example, by day 3 or 4 postinfection, pycnotic and karyorhexic nuclei associated with staining for viral RNA or protein were consistently observed throughout the pyramidal layer of the hippocampus (Fig. 3D). In contrast, in all 30 mice studied which were inoculated in the cortex, neurons in the dentate gyri and cerebella were never positive for virus, neither RNA nor protein, and showed no changes in morphology. Direct inoculation of virus into the cerebellum resulted in infection and cell destruction (Fig. 3B).

GDVII infection of astrocytes and oligodendrocytes was determined by ^{35}S in situ hybridization for viral RNA followed by immunostaining for GFAP or CNPase, phenotypic markers, respectively, of astrocytes and oligodendrocytes. To check the fidelity of the double-labelling technique, adjacent sections were labelled by in situ hybridization only or immunostaining only. The distributions of the in situ hybridization signal and the immunostaining were identical in single- and double-labelled sections.

GDVII RNA-positive $GFAP^+$ cells were detected in the brains and spinal cords of both CBA and BALB/c mice. Only a small proportion of the GDVII-positive cells were $GFAP^+$. GDVII-positive $GFAP^+$ cells with an astrocytic morphology were rare (Fig. 3L). Most double-labelled cells were rounded and did not show typical astrocytic cell processes (Fig. 3M). Infection of astrocytes was lytic, as evidenced by GFAP staining associated with nuclear debris and the absence of morphologically normal astrocytes in areas of widespread infection and cell destruction.

GDVII-positive $CNPase^+$ cells were rare. In areas of limited infection, as evidenced by no extensive cell death and few virus-positive cells with a low density of silver grains, GDVII-positive $CNPase^+$ cells were never observed (Fig. 3E). In these areas, even satellite oligodendrocytes adjacent to infected neurons were consistently virus negative. In areas of extensive infection, with many GDVII-positive cells with a high density of silver grains and widespread cell death, the majority of intact cells remaining could be clearly identified as $CNPase^+$ but were GDVII negative and had the morphological appearance of normal oligodendrocytes (Fig. 3G and H). In these same regions, GDVII-positive $CNPase^+$ cells with a typical oligodendrocyte morphology were rare and CNPase staining in association with nuclear debris was rarely observed (Fig. 3J and I). At no time postinfection were isolated single GDVII-positive $CNPase^+$ cells observed in any part of the CNS.

In situ hybridization signals were never associated with the rod-shaped nuclei characteristic of microglia, even when these cells were adjacent to GDVII-positive cells (Fig. 3K). Attempts to double-label these cells were unsuccessful, even in cryostat sections. Viral RNA and viral protein were never observed in meningeal, ependymal, cerebral endothelial, or choroid plexus cells. In the many sections studied from brains and spinal cords of both CBA and BALB/c mice at days 1 to 5 postinfection, no differences in viral tropism were observed between these mouse strains.

Virus persistence in vivo. To investigate the protective role of the immune system and to determine whether GDVII virus can persist in the CNS, CBA mice were peripherally immunized with heat-inactivated GDVII and 2 weeks later challenged i.c. with GDVII virus. By this time the mice were 8 to 9 weeks old. It was assumed that the chance of establishing a persistent infection would be greatest in mice given a maximal but sublethal i.c. inoculation. In a pilot study of immunized mice, this dose was found to be 100 PFU. Three naive CBA mice and three sham-immunized mice were inoculated with 10^2 PFU of GDVII at 8 to 9 weeks of age. All six mice were dead by day 10 postinoculation. In the experimental group of 45 immunized and infected mice, 10 were sampled on day 7. Of the remaining 35, 20 died (57% mortality) of acute encephalitis between 7 and 17 days postinfection. The 15 survivors were checked weekly for development of signs of chronic demyelinating disease. By day 168 postinfection, none had exhibited clinical signs of disease, and the mice were sampled. The brains

and Purkinje cells in the cerebellum following direct inoculation of virus into this structure. The white matter is at the top, the granule cells form the densely packed middle layer, and the lower layer is the molecular layer. Note pycnotic nuclei of infected cells (arrowheads). The Purkinje cells which should be present between the granule and molecular layers have been destroyed. The large round vacuole between the two arrows may be the remains of a Purkinje cell. (C) Viral RNA-positive motor neurons in the spinal cord. (D) Viral RNA in CA1 hippocampal pyramidal neurons. Extensive cell death with pycnosis, karyorhexis (arrowhead), and nuclear debris is apparent. (E) Viral RNA-negative oligodendrocytes. (F) Viral RNA-positive oligodendrocyte. (G) Viral RNA-negative oligodendrocytes in area of heavy infection. (H) Surviving viral RNA-negative oligodendrocytes in area of widespread destruction as evidenced by the absence of cells and presence of nuclear debris. (I) Area of heavy infection with viral RNA-negative morphologically normal oligodendrocytes. Note the destruction of oligodendrocytes associated with viral RNA (arrowheads). (J) Viral RNA-positive oligodendrocytes in area of widespread destruction. (K) Microglial response, as evidenced by cells of rod-shaped nuclei (arrowhead), adjacent to viral RNA-positive cells. (L and M) Viral RNA-positive astrocytes with process (L) or with shrunken cytoplasm (arrowheads) (M). (O) Virus RNA-positive cells in pyramidal layer of the hippocampus. (P) Viral infection of cerebral cortex, with widespread necrosis. (Q) GDVII RNA-positive cells in the internal capsule. These are arranged in chains (arrowheads), typical of oligodendrocytes in white matter tracts. (R) Submeningeal polymorphonuclear cell infiltrate (arrowhead).

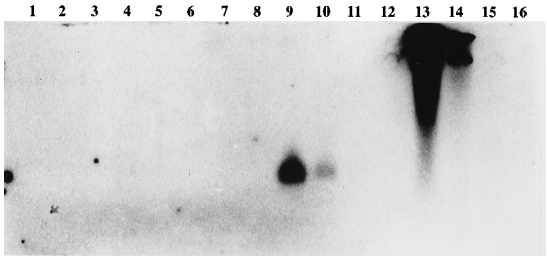

FIG. 4. Southern blot analysis of RT-PCR-amplified GDVII virus sequences derived from brain and spinal cord pooled RNA. The RNA was extracted from mice immunized and subsequently inoculated i.c. Lanes: 1, ϕX174 *Hae*III digest (Southern blot negative control); 2, RT-PCR reagents only, no template RNA; 3 to 8, RT-PCR of RNA from GDVII mice at 168 days postinoculation; 9 to 12, RT-PCR of 10-fold serial dilutions from 1 to 10^{-3} fg of purified GDVII RNA diluted in 100 ng of uninfected total brain RNA; 13 to 16, 10-fold serial dilutions of 1 to 10^{-3} pg of B2 DNA (pGem3 harboring the 3.4-kb *Sal*I-*Xba*I cDNA restriction fragment of BeAn virus) (Southern blot-positive control). Bands were visualized by using the enhanced chemiluminescence detection system with exposure for 90 min. After 150 min, an additional band was visible in lane 11. All experimental samples (3 to 8) were negative for viral RNA.

were divided sagittally, and the spinal cords were divided longitudinally. One half of each sample was processed for histological examination, and the other was processed for RNA extraction. None (0 of 15) of the mice were virus positive by in situ hybridization. Southern blot analysis of RT-PCR products of RNA isolated from the CNS of these mice was also consistently virus negative (Fig. 4). The sensitivity of the RT-PCR was such that three molecules of GDVII genomic RNA diluted in 100 ng of total brain RNA could be reverse transcribed and PCR amplified and the product could be detected by Southern blot hybridization. Taking into account that 1 μg of total CNS RNA was used for RT-PCR and that on average 300 μg of total RNA could be extracted from one brain, the limit of detection of our assay was approximately 900 molecules of GDVII RNA. It has been estimated that during chronic CNS infection with DA virus, the majority of infected cells contain 100 to 500 copies of the viral genome (5). This would imply that the limit of detection of our RT-PCR technique was approximately 9 to 2 persistently infected cells per brain.

DISCUSSION

Following i.c. inoculation of CBA and BALB/c mice, GDVII replicated to high titers, producing an acute fatal encephalomyelitis from which all mice died by day 5. Viral RNA was consistently detected in some areas and was consistently absent in others. There was marked destruction of neurons and astrocytes but only rarely of oligodendrocytes and only in areas of widespread infection. The pattern of infection was consistent both with cell-to-cell spread, presumably as a result of local release of infectious virus around cell bodies, and with the spread of infection between distant areas connected by neuronal pathways. Infection of cortical and basal ganglia neurons, the early infection of spinal cord motor neurons, and the presence of viral RNA and proteins in neuronal processes are consistent with the spread of GDVII along corticospinal tracts. Hematogenous spread of TMEV has been proposed on the basis of the observation that viral RNA can be observed in cells associated with the vascular endothelium in the CNS (50). In the present study, GDVII RNA was not detected in endothelial or choroid plexus cells. Given the mechanism of GDVII spread, it was notable that some neurons were consistently negative for viral RNA, indicating an inability either to reach, to infect, or to replicate within these cells. The most striking examples were the dentate gyrus, which remained negative for viral RNA, despite heavy infection of adjacent hippocampal pyramidal neurons; the majority of thalamic nuclei, which were virus negative despite infection of connecting cortical neurons; and the cerebellum. In the case of the cerebellum, direct inoculation of virus demonstrated that the cells in this structure are not refractory to infection and can replicate virus. The consistent absence of virus-positive cells in this structure is therefore likely to have resulted from a failure of virus to enter or to traffic along cerebellar pathways before the mice died. That infection of susceptible neuronal populations depends on the route of inoculation has also been demonstrated in the olfactory nuclei with the DA strain of TMEV (49). The consistent absence of infection in specific areas such as the cerebellum which contain permissive cells would also argue against, at least random, hematogenous spread of virus.

In previous studies, GDVII was detected exclusively in neurons (27, 45). To investigate glial cell tropism, we developed a highly sensitive double-labelling technique in which in situ hybridization preceded immunocytochemistry. This was in contrast to most double-labelling studies in which this combination was used in reverse order. This is the first study to demonstrate GDVII infection of glial cells in vivo. GDVII RNA-positive cells were predominantly neurons as determined by morphology and location. Although fewer than virus-positive neurons, astrocytes positive for viral RNA were also readily observed. Infected oligodendrocytes were rare but nevertheless present. The explanation for the low frequency of GDVII RNA-positive oligodendrocytes is not immediately apparent but could depend on the access to, binding to, entry into, or replication within these cells or a combination of these. That viral RNA was detected in oligodendrocytes, even satellite oligodendrocytes, only in well-developed lesions could indicate that these cells were infected only at late time points. Whereas this could be the case in white matter tracts where inflammation, axonal loss, or myelin damage could be a prerequisite for widespread access of virus to these compact areas, it would seem less likely for oligodendrocytes in the grey matter. Attachment or entry of virus into oligodendrocytes could be less efficient than for other cell types and could result, for example, from constitutive low or only inducible expression of the viral receptor or inefficient endocytosis. Finally, GDVII replication could be restricted in oligodendrocytes as previously described for DA virus (5 to 7). In this case, oligodendrocytes could even be infected at the same time and with the same efficiency as other cell types, but viral RNA would become detectable only as transcripts slowly accumulated with time and virus-positive cells would be observed only rarely and in late lesions. With time, or perhaps in response to changes in, for example, the external cytokine or physical environment, changes in the physiology of the infected oligodendrocyte could lead to upregulation of the viral receptor or enhanced virus replication. That activation and/or differentiation states of cells can affect virus replication has been shown for several systems including glial cells (11–13, 19, 33, 37).

In our studies of BeAn tropism (43, 44) and those of others with DA (1), viral RNA-positive oligodendrocytes are observed only weeks after infection. In oligodendrocytes, GDVII RNA can therefore be detected earlier than TO strain RNA. Given the widespread nature of GDVII infection relative to BeAn or DA infection (43, 44), this could result from the increased chance of observing a rare event such as virus entry into or unrestricted replication within an oligodendrocyte. Alternatively, it could reflect more efficient entry or replication, even restricted replication, of GDVII relative to BeAn. Whether complete replication of virus in oligodendrocytes is

destructive is not clear for either GDVII or TO strains. Destruction of GDVII-infected oligodendrocytes was rare and observed only in areas of widespread infection with destruction of surrounding cells, an environment in which it is impossible to determine the cause of the demise of the GDVII-positive oligodendrocytes.

Our demonstration that GDVII can infect glial cells in vivo, together with recent studies indicating that both virulent and avirulent subgroups of TMEV encode genetic determinants of demyelination (17), led us to investigate whether GDVII can persist in the CNS. In CBA mice, susceptible to TO virus persistence, immunization prior to infection with GDVII protected mice from lethal acute encephalomyelitis; however, by 168 days postinfection all survivors had cleared infection from the CNS as detected by both in situ hybridization and RT-PCR. These results are in agreement with recent studies using chimeric GDVII and DA viruses which indicated that GDVII does not contain genetic determinants of persistence and does not cause chronic demyelinating disease (20, 24). Our results clearly indicate that the inability of GDVII to persist does not result from an inability to infect oligodendrocytes. However, as with TO strains, infection of these cells relative to neurons and astrocytes is either less efficient or restricted or both. In mice resistant to TO virus persistence, $CD8^+$ T cells play a dominant role in clearing virus from the CNS (2, 4, 15, 22, 23, 34, 40). The ability of mice susceptible to TO virus persistence to clear GDVII could result from the ability of GDVII to elicit an effective immune response, which could result, for example, from a difference in T-cell epitopes, in particular those in VP1.

ACKNOWLEDGMENTS

We are grateful to William F. Blakemore for useful discussions.

This research was supported by a grant to J.K.F. from the British Multiple Sclerosis Society and a research fellowship to J.P.S. from the National Board for Scientific and Technological Research, Portugal.

REFERENCES

1. **Aubert, C., M. Chamorro, and M. Brahic.** 1987. Identification of Theiler's virus infected cells in the central nervous system of the mouse during demyelinating disease. Microb. Pathog. **3:**319–326.
2. **Azoulay, A., M. Brahic, and J.-F. Bureau.** 1994. FVB mice transgenic for the *H-2D^b* gene become resistant to persistent infection by Theiler's virus. J. Virol. **68:**4049–4052.
3. **Blakemore, W. F., C. J. Welsh, P. Tonks, and A. A. Nash.** 1988. Observations on demyelinating lesions induced by Theiler's virus in CBA mice. Acta Neuropathol. **76:**581–589.
4. **Borrow, P., P. Tonks, C. J. R. Welsh, and A. A. Nash.** 1992. The role of CD8+ T cells in the acute and chronic phases of Theiler's murine encephalomyelitis virus-induced disease in mice. J. Gen. Virol. **73:**1861–1865.
5. **Cash, E., M. Chamorro, and M. Brahic.** 1985. Theiler's virus RNA and protein synthesis in the central nervous system of demyelinating mice. Virology **144:**290–294.
6. **Cash, E., M. Chamorro, and M. Brahic.** 1986. Quantitation, with a new assay, of Theiler's virus capsid protein in the central nervous system of mice. J. Virol. **60:**558–563.
7. **Cash, E., M. Chamorro, and M. Brahic.** 1988. Minus-strand RNA synthesis in the spinal cords of mice persistently infected with Theiler's virus. J. Virol. **62:**1824–1826.
8. **Chomczynsky, P., and N. Sacchi.** 1987. Single step method of RNA isolation by acid guanidinium thiocyanate-phenol-chloroform extraction. Anal. Biochem. **162:**156–159.
9. **Dal Canto, M. C., and H. L. Lipton.** 1975. Primary demyelination in Theiler's virus infection: an ultrastructural study. Lab. Invest. **33:**626–637.
10. **Dal Canto, M. C., and H. L. Lipton.** 1982. Ultrastructural immunohistochemical localisation of virus in acute and chronic demyelinating Theiler's virus infection. Am. J. Pathol. **106:**20–29.
11. **Dukto, F. J., and M. B. A. Oldstone.** 1981. Cytomegalovirus causes a latent infection in undifferentiated cells and is activated by induction of cell differentiation. J. Exp. Med. **154:**1636–1651.
12. **Embretson, J., M. Zupancic, J. L. Ribas, A. Burke, P. Racz, K. Tenner-Rackz, and A. T. Haase.** 1993. Massive covert infection of helper T lymphocytes and macrophages by HIV during the incubation period of AIDS. Nature (London) **362:**359–362.
13. **Fan, S. T., K. Hsia, and T. S. Edgington.** 1994. Up regulation of HIV-1 in chronically infected monocyte cell line by both contact with endothelial cells and cytokines. Blood **84:**1567–1572.
14. **Fazakerley, J. K., S. Pathak, M. Scallan, S. Amor, and H. Dyson.** 1993. Replication of the A7(74) strain of Semliki Forest virus is restricted in neurons. Virology **195:**627–637.
15. **Fiette, L., C. Aubert, M. Brahic, and C. Peña Rossi.** 1993. Theiler's virus infection of β_2-microglobulin-deficient mice. J. Virol. **67:**589–592.
16. **Frankel, G., A. Friedmann, A. Amir, Y. David, and A. Shahar.** 1986. Theiler's virus replication in isolated Schwann cell cultures. J. Neurosci. Res. **15:**127–136.
17. **Fu, J., M. Rodriguez, and R. P. Roos.** 1990. Strains from both Theiler's virus subgroups encode a determinant for demyelination. J. Virol. **64:**6345–6348.
18. **Fu, J., S. Stein, L. Rosenstein, T. Bodwell, M. Routbort, B. L. Semler, and R. P. Roos.** 1990. Neurovirulence determinants of genetically engineered Theiler's viruses. Proc. Natl. Acad. Sci. USA **87:**4125–4129.
19. **Gonczol, E., P. W. Andrews, and S. A. Plotkin.** 1984. Cytomegalovirus replicates in differentiated but not undifferentiated human embryonal carcinoma cells. Science **224:**159–161.
20. **Jarousse, N., R. A. Grant, J. M. Hogle, L. Zhang, A. Senkowski, R. P. Roos, T. Michiels, M. Brahic, and A. McAllister.** 1994. A single amino acid change determines persistence of a chimeric Theiler's virus. J. Virol. **68:**3364–3368.
21. **Lehrich, J. R., B. G. W. Arnason, and F. H. Hochberg.** 1976. Demyelinative myelopathy in mice induced by the DA virus. J. Neurol. Sci. **29:**149–160.
22. **Lindsley, M. D., and M. Rodriguez.** 1989. Characterisation of the inflammatory response in the central nervous system of mice susceptible or resistant to demyelination by Theiler's virus. J. Immunol. **142:**2677–2682.
23. **Lindsley, M. D., R. Thiemann, and M. Rodriguez.** 1991. Cytotoxic T cells isolated from the central nervous system of mice infected with Theiler's virus. J. Virol. **65:**6612–6620.
24. **Lipton, H. L., M. Calenoff, P. Bandyopadhyay, S. D. Miller, M. C. Dal Canto, S. Gerety, and K. Jensen.** 1991. The 5′ noncoding sequences from a less virulent Theiler's virus dramatically attenuate GDVII neurovirulence. J. Virol. **65:**4370–4377.
25. **Lipton, H. L.** 1975. Theiler's virus infection in mice: an unusual biphasic disease process leading to demyelination. Infect. Immun. **11:**1147–1155.
26. **Lipton, H. L.** 1980. Persistent Theiler's murine encephalomyelitis virus infection in mice depends on plaque size. J. Gen. Virol. **46:**169–177.
27. **Liu, C., J. Collins, and E. Sharp.** 1967. The pathogenesis of Theiler's GDVII encephalomyelitis virus infection in mice as studied by immunofluorescent technique and infectivity titrations. J. Immunol. **98:**46–55.
28. **Maniatis, T., E. F. Fritsch, and J. Sambrook.** 1982. Molecular cloning: a laboratory manual. Cold Spring Harbor Laboratory, Cold Spring Harbor, N.Y.
29. **O'Hara, Y., H. Konno, Y. Iwasaki, T. Yamamoto, H. Terunuma, and H. Suzuki.** 1990. Cytotropism of Theiler's murine encephalomyelitis viruses in oligodendrocyte-enriched cultures. Arch. Virol. **114:**293–298.
30. **O'Hara, Y., S. Stein, J. L. Fu, L. Stillman, L. Klaman, and R. P. Roos.** 1988. Molecular cloning and sequence determination of DA strain of Theiler's murine encephalomyelitis viruses. Virology **164:**245–255.
31. **Olitsky, P. K.** 1945. Certain properties of Theiler's virus, especially in relation to its use as a model for poliomyelitis. Proc. Soc. Exp. Biol. Med. **58:**77–81.
32. **Ozden, S., F. Tangy, M. Chamorro, and M. Brahic.** 1986. Theiler's virus genome is closely related to that of encephalomyocarditis virus, the prototype cardiovirus. J. Virol. **60:**1163–1165.
33. **Pasick, J. M. M., and S. Dales.** 1991. Infection by coronavirus JHM of rat neurons and oligodendrocyte-type-2 astrocyte lineage cells during distinct developmental stages. J. Virol. **65:**5013–5028.
34. **Pena Rossi, C., A. McAllister, L. Fiette, and M. Brahic.** 1991. Theiler's virus infection induces a specific cytotoxic T lymphocyte response. Cell. Immunol. **138:**341–348.
35. **Pevear, D. C., J. Borkowski, M. Calenoff, C. K. Oh, B. Ostrowski, and H. L. Lipton.** 1988. Insights into Theiler's virus neurovirulence based on a genomic comparison of the neurovirulent GDVII and less virulent BeAn strains. Virology **165:**1–12.
36. **Pevear, D. C., M. Calenoff, E. Rozhon, and H. L. Lipton.** 1987. Analysis of the complete nucleotide sequence of the picornavirus Theiler's murine encephalomyelitis virus indicates that it is closely related to cardioviruses. J. Virol. **61:**1507–1516.
37. **Poly, G., A. L. Kinter, and A. S. Fauci.** 1994. Interleukin-1 induces expression of HIV alone and in synergy with interleukin-6 in chronically infected U1 cells: inhibition of inductive effects by the interleukin-1 receptor antagonist. Proc. Natl. Acad. Sci. USA **91:**108–112.
38. **Raible, D. W., and F. A. McMorris.** 1989. Cyclic AMP regulates the rate of differentiation of oligodendrocytes without changing the lineage commitment of their progenitors. Dev. Biol. **133:**437–446.
39. **Rodriguez, M., J. L. Leibowitz, and P. W. Lampert.** 1983. Persistent infection of oligodendrocytes in Theiler's virus induced encephalomyelitis. Ann. Neurol. **13:**426–433.
40. **Rodriguez, M., S. Pedrinaci, and C. S. David.** 1993. Abrogation of resistance

to Theiler's virus induced demyelination in H-2b mice deficient in β2-microglobulin. J. Immunol. **151:**266–276.
41. **Rodriguez, M., and R. P. Roos.** 1992. Pathogenesis of early and late disease in mice infected with Theiler's virus, using intratypic recombinant GD-VII/DA viruses. J. Virol. **66:**217–225.
42. **Shahar, A., G. Frankel, Y. David, and A. Friedmann.** 1986. In vitro cytotoxicity and demyelination induced by Theiler's virus in cultures of spinal cord lysis. J. Neurosci. Res. **16:**671–681.
43. **Simas, J. P., S. Amor, A. A. Nash, and J. K. Fazakerley.** Neuroanatomical distribution, spread and tropism of the BeAn strain of TMEV. Submitted for publication.
44. **Simas, J. P., and J. K. Fazakerley.** Molecular analysis of persistence, tropism, and genetic variability of the BeAn strain of Theiler's virus in the mouse CNS. Submitted for publication.
45. **Stroop, W. G., J. R. Baringer, and M. Brahic.** 1981. Detection of Theiler's virus RNA in mouse central nervous system by in situ hybridization. Lab. Invest. **45:**504–509.
46. **Tangy, F., A. McAllister, C. Aubert, and M. Brahic.** 1991. Determinants of persistence and demyelination of the DA strain of Theiler's virus are found only in the VP1 gene. J. Virol. **65:**1616–1618.
47. **Theiler, M.** 1937. Spontaneous encephalomyelitis, a new virus disease. J. Exp. Med. **65:**705–719.
48. **Theiler, M., and S. Gard.** 1940. Encephalomyelitis of mice. III. Epidemiology. J. Exp. Med. **79:**79–90.
49. **Wada, Y., and R. S. Fujinami.** 1993. Viral infection and dissemination through the olfactory pathway and the limbic system by Theiler's virus. Am. J. Pathol. **143:**221–229.
50. **Wada, Y., M. L. Pierce, and R. S. Fujinami.** 1994. Importance of amino acid 101 within capsid protein VP1 for modulation of Theiler's virus-induced disease. J. Virol. **68:**1219–1223.

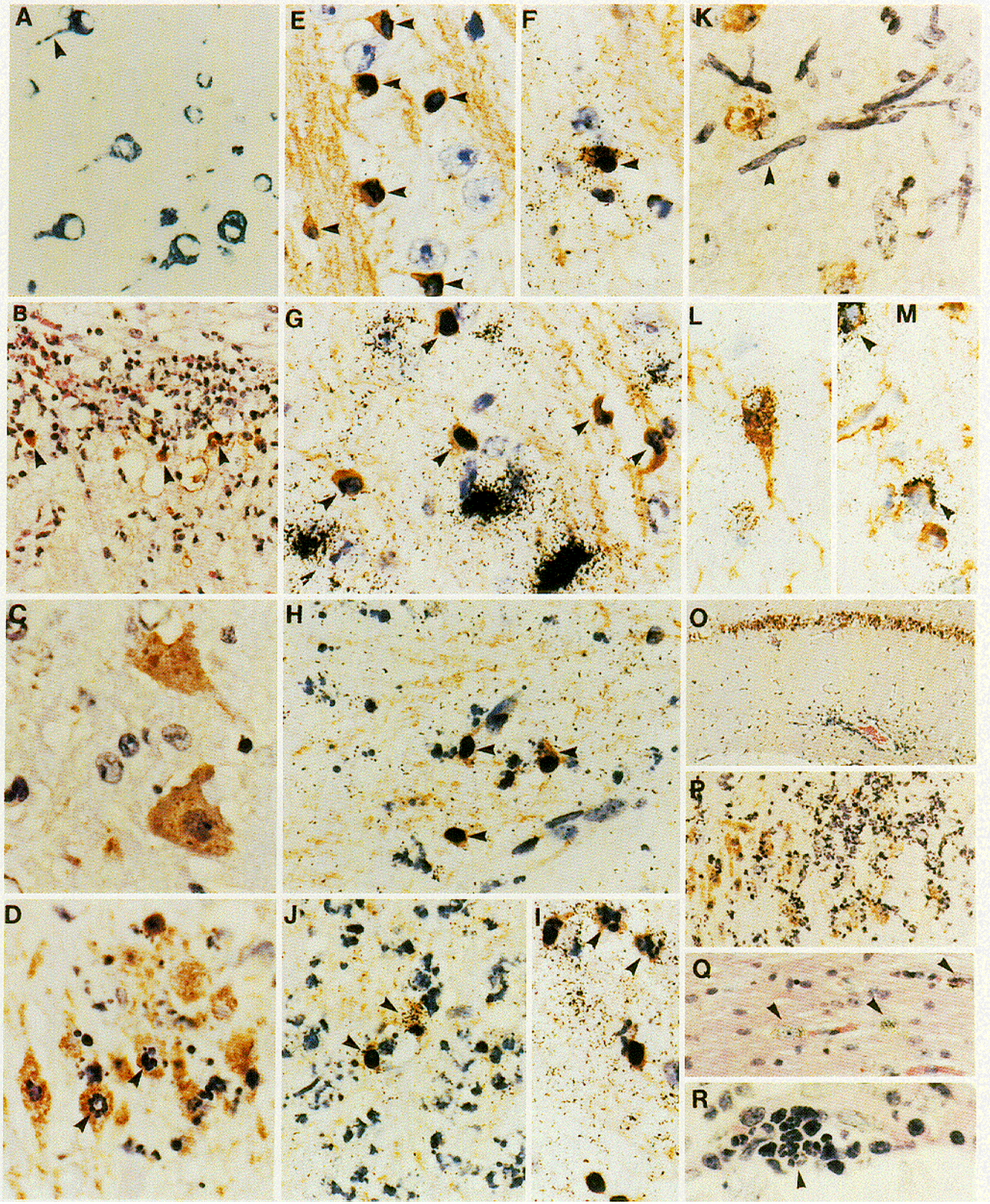
A
E
F
K
B
G
L
M
C
H
O
P
D
J
I
Q
R